ACS Partner Journal

Journal of the American Society for Mass Spectrometry

pubs.acs.org/jasms

Research Article

Resolving Isomers of Star-Branched Poly(Ethylene Glycols) by IMS-MS Using Multiply Charged Ions

Calvin A. Austin, Ellen D. Inutan, Brian C. Bohrer, Jing Li, Joshua L. Fischer, Kanchana Wijerathne, Casey D. Foley, Christopher B. Lietz, Daniel W. Woodall, Lorelie F. Imperial, David E. Clemmer, Sarah Trimpin, and Barbara S. Larsen*

Cite This: https://dx.doi.org/10.1021/jasms.0c00045

Read Online

ACCESS | Metrics & More | Article Recommendations | Supporting Information

ABSTRACT: Ion mobility spectrometry (IMS) mass spectrometry (MS) centers on the ability to separate gaseous structures by size, charge, shape, and followed by mass-to-charge (m/z). For oligomeric structures, improved separation is hypothesized to be related to the ability to extend structures through repulsive forces between cations electrostatically bonded to the oligomers. Here we show the ability to separate differently branched multiply charged ions of star-branched poly(ethylene glycol) oligomers (up to 2000 Da) regardless of whether formed by electrospray ionization (ESI) charged solution droplets or from charged solid particles produced directly from a surface by matrix-assisted ionization. Detailed structural characterization of isomers of the star-branched compositions was first established using a home-built high-resolution ESI IMS-MS instrument. The doubly charged ions have well-resolved drift times, achieving separation of isomers and also allowing differentiation of star-branched versus linear oligomers. An IMS-MS "snapshot" approach allows visualization of architectural dispersity and (im)purity of samples in a straightforward manner. Analyses capabilities are shown for different cations and ionization methods using commercially available traveling wave IMS-MS instruments. Analyses directly from surfaces using the new ionization processes are, because of the multiply charging, not only associated with the benefits of improved gas-phase separations, relative to that of ions produced by matrix-assisted laser desorption/ionization, but also provide the potential for spatially resolved measurements relative to ESI and other ionization methods.

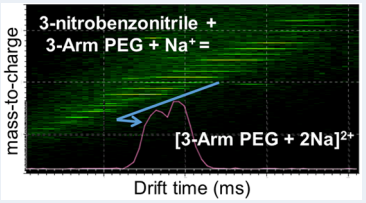

INTRODUCTION

Star-branched polymers were synthesized because of their unique physical properties and their use in a variety of products, including food packaging, drug delivery capsules, and automobile parts.[1−3] The degree of branching allows tuning of the cure time, swelling capacity, tensile strength, and elasticity for specific applications. Star-branched polymers are often prepared through a divergent growth process in which arms are grown outwardly from a core with the number of arms determined by the type of core.[4−6] For example, a pentaerythritol core can be used to synthesize 4-arm star-branched polymers[7,8] and glycerol for 3-arm.[8] A variety of factors influence the growth including temperature, solvent polarity, and reaction site, in theory, allowing monomers to add symmetrically to each arm.[9] Steric hindrance of neighboring arms, however, may cause asymmetric arm growth, resulting in architectural dispersity.[9,10] Detailed characterization of the three-dimensional (3-D) architecture of star-branched polymers is difficult or impossible using well-established polymer methods. Light scattering, size exclusion chromatography, and viscometry, or a combination, are employed in determining *average* properties of polymer architectures such as polymer size and shape.[11−17] Methods such as (ultra)high resolution mass spectrometry (MS) coupled with MS/MS have demonstrated structural characterization in complex polymeric samples.[18,19] These methods are limited to specific polymer compositions such as the presence of a fragile linker group for differentiation of block copolymer arm length.[20]

Ion mobility spectrometry (IMS) coupled to MS has been extensively used to obtain insights into gas-phase macromolecular structures including those of synthetic polymers using home-built instruments.[21−27] IMS separates gas-phase ions by their mobility through a drift gas which is dependent on the collision cross-section (size, shape, and number of charges). IMS-MS data are typically represented as a 2-dimensional (2-D) plot of drift time (t_d) versus the mass-to-charge (m/z) ratio in which ion intensity is embedded as a false color plot. This concept is based on the nested data set of t_d (m/z)[28] correlating two gas-phase separation dimensions, in analogy to the correlation of peaks in a total ion chromatogram and mass spectra in liquid chromatography-MS. Within a 2-D plot, signals for a given m/z represent different structures with differing

Special Issue: Focus: Ionization Technologies Used in MS: Fundamentals and Applications

Received: February 12, 2020
Revised: June 4, 2020
Accepted: June 8, 2020
Published: June 8, 2020

mobility which arrive at the detector at slightly different times.[29] IMS-MS/MS have been employed to differentiate closely related structures.[30] Computational modeling can be used to assist in deciphering the 3-D structure of a specific macromolecule based on drift time measurements.[31−39] Using an IMS-IMS-MS approach, collision-induced activation experiments have been applied to determine, alter, and monitor gas-phase conformations.[34−36]

Early work applied electrospray ionization (ESI)-IMS-MS to the characterization of linear poly(ethylene glycol) (PEG) of increasing size and complexity demonstrated baseline-separated charge-state distributions for a molecular weight (MW) of 6700 Da (PEG-6700).[23] It was shown that a relatively small polymeric system with 30 monomer units formed a compact structure with two cations $[M_{30} + 2Cat]^{2+}$ and an elongated structure with three cations $[M_{30} + 3Cat]^{3+}$ attached. An extended, near-linear structure ("beads-on-a-string") PEG ion with 126 monomer units binding 9 cations $[M_{126} + 9Cat]^{9+}$ was also observed.[23] These experimental and computational results were explained based on Coulombic repulsion of neighboring cations, which stretch the gas-phase PEG ions into an increasingly linear structure enabling the clean separation of charge states ranging from 2 to 10. Subsequent work[24] demonstrated that some oxygen-rich polymers, such as PEG, reveal an inverse relationship between mobility and charge states, contrary to that observed for biopolymers (proteins)[40−43] and with other polymers.[24] Sigmoidal transitions relate to extended to folded structures. These transitions are only observed above a certain polymer size, which upon folding behave more typical of compact charge-state relationships common to biopolymers (proteins). ESI-IMS-MS has also been used to study the mechanism of PEG-11000 ion formation, expanding on why certain polymer lengths acquire a specific number of charges and how charges may be gained or lost.[25]

The utility of an IMS gas-phase separation dimension combined with gas-phase MS m/z separation using commercially available IMS-MS instruments has been demonstrated in a number of areas.[44−47] Increasing the charge states for polymer samples has been shown to enhance separations.[44,45,48] Particularly relevant to this work is a more recent ESI-IMS-MS study that demonstrated the first example of distinguishing between symmetric and asymmetric star-branched and linear PEG polymers.[48]

A number of newer ionization methods have been used for polymer analyses other than the traditional ESI and MALDI methods,[49−52] such as the atmospheric solid analysis probe (ASAP) method for sufficiently volatile oligomers and additives.[53−55] Initial proof-of-principle of new ionization processes, that lead to the Biemann Medal in 2019, for use with MS and IMS-MS have also been reported for oligomer analyses.[56,57] The ability to generate multiply charged ions similar to ESI directly from surfaces has been demonstrated.[58−60] The ionization process is assisted by temperature, pressure, and the associated collisions, in addition to the matrix or solvent used to dissolve the analyte of interest.[61−65]

Here, a home-built ESI-IMS-MS instrument with high drift time resolution[34−36,66] was used to unravel the architectural differences of isomeric PEG-based star-branched polymers having asymmetries based on arm lengths. The potential use of unique 2-D pictorials for fast characterization of specific polymeric architectures within a single sample is demonstrated. Similar analyses of the polymer samples were made using the traveling wave IMS (TWIMS) (Waters SYNAPT G2) instrument using ESI and newer ionization methods that produce multiply charged ions.

EXPERIMENTAL SECTION

Instrumentation. A home-built instrument (Scheme S1) that incorporates ESI with IMS and MS was used for all experiments.[34−36,67] Here, a brief description is provided. The IMS-IMS-IMS-MS instrument contains four ion funnels (F1, F2, F3, F4), three ion gates (G1, G2, G3), and three activation regions (A1, A2, A3). A continuous beam of ions is accumulated with an electrostatic ion gate at the end of the first ion funnel. Lowering the gate allows a short pulse of ions to enter the drift region filled with He buffer gas. All m/z values are determined using an orthogonal reflectron time-of-flight (TOF) analyzer.[28] IMS-IMS-MS is used to activate drift time selected ions. The 2-D plots of t_d (m/z) are generated with Origin Software 6.1 and 7.0 (OriginLab Corp, Northampton, MA 01060) and processed using slicing software written in-house.[28] The multidimensional output generated using IMS-MS is expressed using nested data sets displayed as t_d (m/z).[23,24,28]

The Waters SYNAPT G2 and G2S incorporate a TRI-WAVE ion mobility region. The drift times were extracted for the specific mass-to-charge m/z values. DriftScope was used to view the 2-dimensional plot of drift time versus m/z (snapshot).

Ionization Sources and Methods. On the home-built IMS-MS instrument, ESI was used.[23,24] A Thermo LTQ Orbitrap classic with ESI was used. The Waters SYNAPT G2 and G2S IMS-MS instruments are equipped with various interchangeable commercial and home-built sources for ESI, vacuum MALDI, laserspray ionization (LSI), matrix assisted ionization (MAI), and vacuum MAI (νMAI). νMAI was achieved using a commercial intermediate pressure vacuum MALDI source of the Waters SYNAPT G2 and simple source modifications that in particular reduce voltages and eliminate the necessity of a laser.[68]

The MS prototype vacuum-probe vMAI source[69] was used with the SYNAPT G2S for robust and prompt ionization. The vacuum-probe assembly was designed to interface with the SYNAPT G2 and G2S (Waters) in which the commercial ESI inlet is replaced with the newly designed prototype single vacuum-probe device. The new ionization processes produce multiply charged ions from surfaces without the necessity for using a laser, voltage, or heat for analyte ionization,[61−65] although these means can be used (e.g., LSI). In the νMAI experiment, the matrix, analyte, and salt are cocrystallized, briefly dried prior to sample introduction, as described below. The probe is introduced into the vacuum of a mass spectrometer where ionization commences without any additional energy input. The cationized polymer ions are spontaneously formed and transmitted toward the mass analyzer.

Materials and Sample Preparation. Linear PEG-970 and different 3- and 4-arm star-branched PEG polymers star-branched 4-arm (PEG-800 and PEG-2000), 3-arm (PEG-1000) were provided by DuPont. Polymer solutions of concentrations 0.25 mg·mL^{-1} in 1:1 (v:v) water/acetonitrile containing 1 M lithium chloride (Sigma-Aldrich) were prepared for all experiments according to previous work using ESI.[23] The typical MALDI matrix, 2,5-dihydroxybenzoic acid (2,5-DHB), LSI matrix 2,5-dihydroxyacetophenone (2,5-DHAP), and MAI matrix 3-nitrobenzonitrile (3-NBN) were obtained from Sigma-Aldrich.

For all comparisons, sample preparation was kept similar to that of ESI using the same samples and solvents. Salt, analyte,

https://dx.doi.org/10.1021/jasms.0c00045
J. Am. Soc. Mass Spectrom. XXXX, XXX, XXX−XXX

Scheme 1. Illustrations of Branched PEG Polymer: (A) 4-Arm and (B) 3-Arm

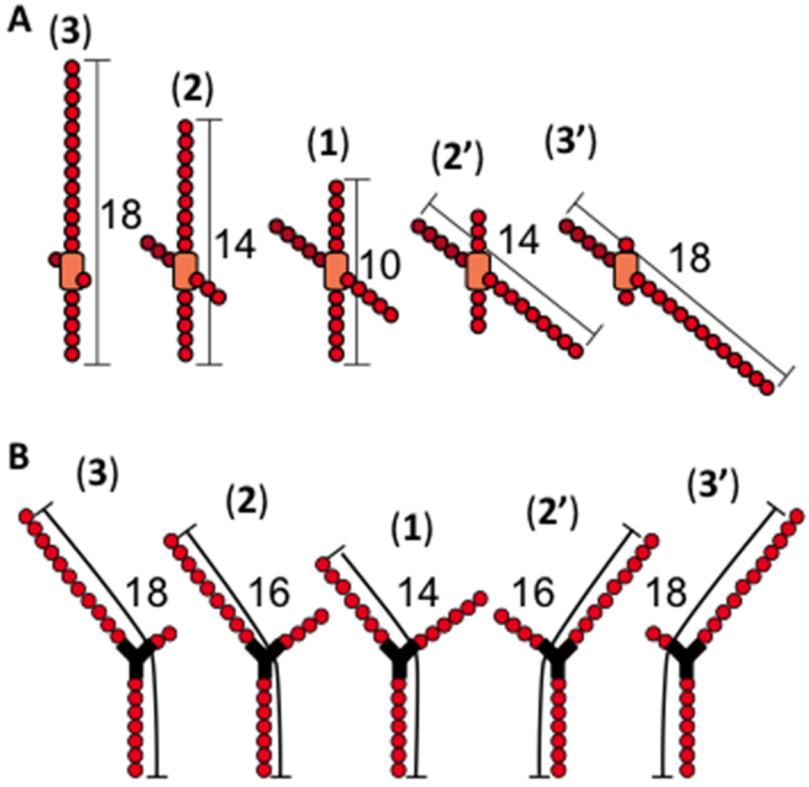

and MALDI matrix (2,5-DHB) or MAI matrix (3-NBN) were dissolved individually and mixed. Typically, the matrix/PEG/salt molar ratio was 5600:1:100 using the 3-NBN matrix and sodium or lithium trifluoroacetate salts. PEG samples (typically, 20 pmol μL^{-1} in 1:1 acetonitrile/water) were mixed in equal volumes with an aqueous salt solution (1 mg mL^{-1}) and a matrix (0.1 mg mL^{-1} in 2,5-DHB in water, and 3-NBN in acetonitrile). The solution was briefly vortexed, and typically 1 μL of the solution was used in the dried droplet fashion for both MALDI and MAI using the commercial vacuum MALDI source with and without engaging the laser, respectively. Alternatively, the analyte, salt, and matrix solution may be applied in a layered fashion without being previously mixed. Note: improved *v*MAI results using the vacuum-probe were obtained using higher concentrated salt solution directly applied to the probe tip; this is without concern because the nonvolatile salts remain on the probe.[64,68,69]

RESULTS AND DISCUSSION

Statistical Considerations of the Synthesis of Star-Branched Polymers. The synthesis of the commercial star-branched polymers is proprietary. Therefore, the initial interpretation begins with certain assumptions for the effect of branching on the drift time and m/z data sets obtained by IMS-MS of the various star-branched polymers. The synthesis of these branched polymers follows a divergent growth process, where the addition of a new monomer can occur on any of the arms with a probability inversely proportional to the number of arms, resulting in structural isomers. For PEG polymers with more than two arms (Scheme 1), the probability of monomer addition to any arm is statistically equivalent resulting in symmetric structures with higher probability than asymmetric structures. This is exemplified in the following. For illustration, the branched polymers depicted each have 20 repeat units and distributed over four (Scheme 1A) and three arms (Scheme 1B). In the most asymmetric and truncated case, a 4-arm star-polymer will have only two short arms grown with two long arms (Scheme 1A (3) and A (3′)), or in the most symmetric isomer case 4-arms grown with five repeating units each (Scheme 1A(1)). The same principal is depicted for the 3-arm in Scheme 1B. The MW of any of these variations is the same within A or B but different between samples (A versus B) because of the differences in the core structures.

The samples used in this study have an *average* size difference of 200 Da, which corresponds to 4.5 more monomer units for the PEG-1000 than for the PEG-800 sample. In the m/z separation using MS, the 3-arm PEG with its longer arm's is expected to have higher charge states than the 4-arm. This is, for example, observed with a high resolution mass spectrometer (Scheme S1) for a 4-arm PEG-800 sample versus 3-arm PEG-1000 star-branched polymer. Nothing can be determined about the architectural composition by the observed charge states.

For PEG polymers, it has been shown that approximately seven repeats are needed to stabilize each charge.[23] For the star-branched polymers studied here, the doubly charged ions with arms of equal length are likely to have two cations bound to two different arms (Scheme 2A). On the basis of the beads-on-a-string concept,[23,24] the gas-phase ions of isomeric structures of longer chains will extend to a greater length than those of shorter chains of multiply charged star-branched polymers having at least two monovalent cations (here, lithium cations) (Scheme 2B). Specifically, we hypothesized that the near-linear, asymmetric structures of the same star-branched polymer (cases (**3**) and (**3′**) in Scheme 1) will show increased elongation over the symmetric structures (cases (**1**) in Scheme 1). While the MW is the same, the different degree of elongation each

https://dx.doi.org/10.1021/jasms.0c00045
J. Am. Soc. Mass Spectrom. XXXX, XXX, XXX−XXX

Scheme 2. Illustrations of Binding of Two Lithium Ions to 4-Arm Branched PEG Polymer Symmetrically and Asymmetrically

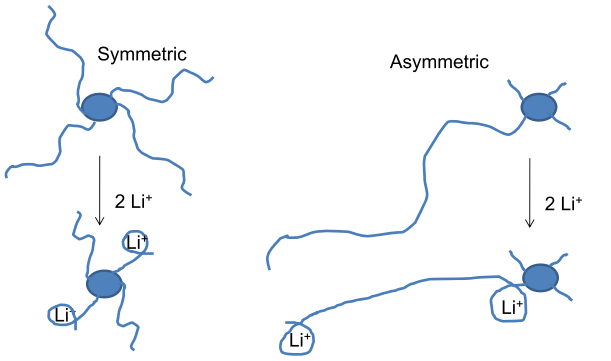

multiply charged isomer can adopt is likely key in their separation by IMS. The expectation is that only isomeric structures in which the two longest arms lead to different length extended structures can be separated with the IMS-MS technology currently available. The 4- and 3-arm star-branched structures of nearly identical shape will be indistinguishable from each other, e.g. two additional monomers on positions one and two versus on one and three. Singly charged isomers more likely adopt globular structures regardless of the isomers' differences in arm-length, and separation of these isomers is therefore more difficult to achieve.

Predicting the ability to separate a 4- from a 3-arm star polymer with exactly the same number of arm lengths, as is shown in Scheme 1 for a sum of 18 repeat units, will likely depend to some extent on the influence of the core. However, the likelihood of asymmetric structures **B** (**3**) and **B** (**3′**), in which three monomer units contribute to elongation, is much greater than that of structure **A** (**3**) and **A** (**3′**) in which the statistically unlikely alteration must accrue eight monomer units. Therefore, we must expect that the extended structures for the 3-arm relative to that of the 4-arm are much more likely to be chemically synthesized and therefore more abundant.

The following sections discuss the ability of separating architectural differences by IMS-MS. For our strategy, we first used ionization conditions that have been studied in detail for cation attachments of linear polymers, including those of statistical polymers, and were studied using IMS-MS in the past with home-built instruments.[23,24] Using Li^+ cations for attaching to the relatively short arm-length was a reasonable assumption to provide good analytical results that would serve as a means of validating subsequent results on the commercially available IMS-MS instruments. On the commercial IMS-MS instruments, we varied the conditions including those that led to the formation of singly (MALDI) and multiply charged ions (ESI and new ionization methods).

Homebuilt ESI-IMS-MS: Different Branched Polymers. *4-Arm Star-branched PEG-800.* The 4-arm star-branched PEG-800 doped with lithium chloride reveals, in the 2-D plot of IMS-MS, a family of singly charged ions within the nested data set of t_d (m/z) ~33(538) to ~50(1019), with each m/z having an associated drift time distribution of ca. 2 ms (Figure 1A). Extracting the drift time information on specific m/z's reveals no specific (useful) features (Figure S2), indicating that separation of the expected isomers is not achieved based on the singly charged ions.

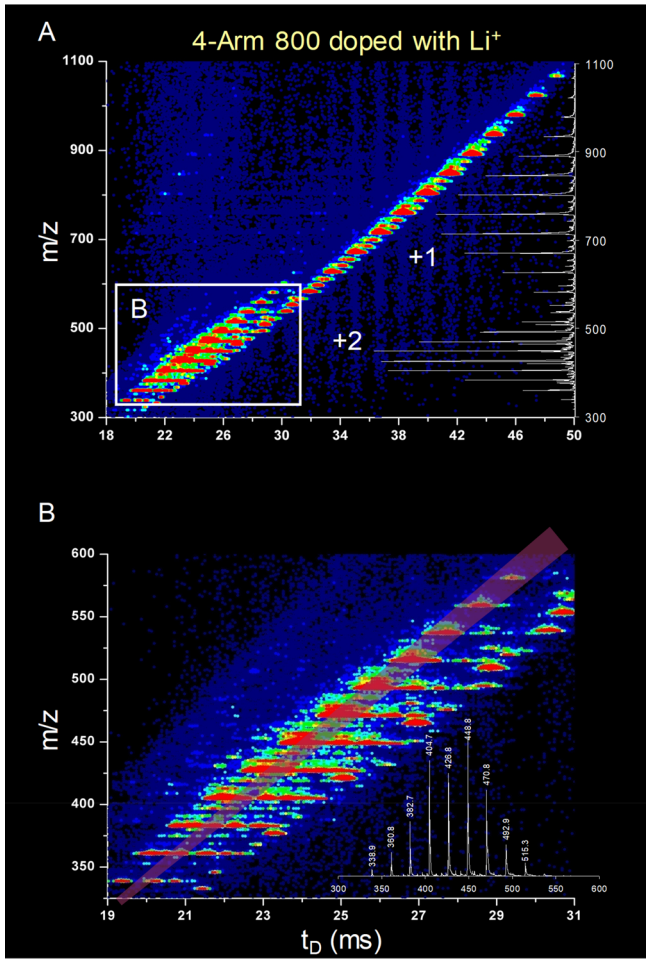

Figure 1. 4-Arm star-branched PEG-800 doped with lithium chloride using home-built IMS-MS. 2-D plot of (A) full range including total mass spectrum and (B) inset regions including one of the extracted mass spectra (for complete data set refer to the Supporting Information). Ion intensities are represented with a false color scale where blue is the lowest intensity, ranging through green to yellow to red, which is the highest intensity.

A family of doubly charged ions is observed from t_d (m/z) ~19(338) to ~31(624) (Figure 1A). In the inset display of the doubly charged family (Figure 1B), each m/z has an associated drift time distribution of ca. 4 ms. These unusually wide drift time distributions result from specific isotopically resolved structures at different m/z values. A more detailed analysis is obtained by extracting specific m/z's from the data set. Here, for the first time, the extracted drift time distributions show separated isomeric star-branched polymers (Figure 2). For example, the extracted doubly charged ions of m/z 338 reveals three abundant drift time distributions along with a low-abundant distribution at the longest drift time all almost baseline separated. Assuming the core is pentaerythritol (MW 136), the doubly charged ion $[M + 2Li]^{2+}$ at m/z 338, having MW 662 Da, would contain 12 repeat units. There is the statistical possibility that more than four isomers have been formed for this specific m/z, which could either mean that families of isomers with similar drift times are separated rather than necessarily individual isomers, or that some of the more asymmetric isomers are of very low abundance. This latter possibility is supported by a lowest-abundance architecture at the longest drift time. The drift time distribution extracted for each m/z in

https://dx.doi.org/10.1021/jasms.0c00045
J. Am. Soc. Mass Spectrom. XXXX, XXX, XXX−XXX

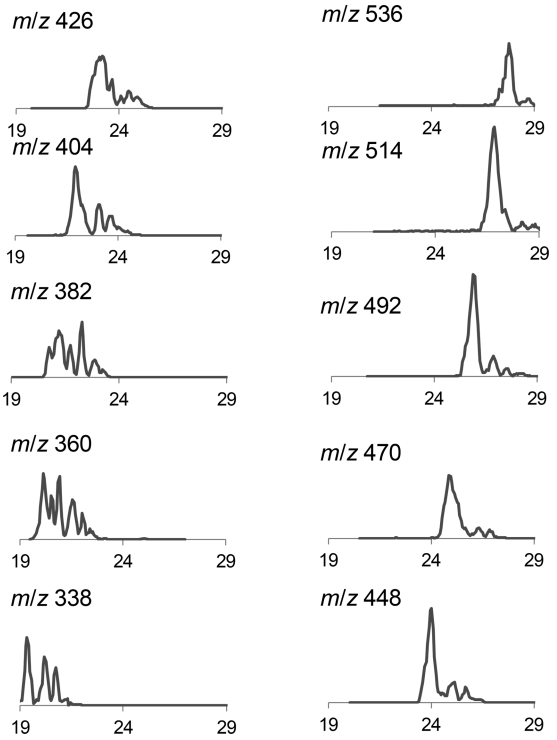

Figure 2. Extracted drift time distributions for the doubly charged 4-arm star-branched PEG-800 doped with lithium chloride using home-built IMS-MS with the specific m/z 338 to 536.

the doubly charged family shows that the shortest drift times are highest in ion abundance (Figure 2), suggesting that isomers with more compact and symmetric structures are present in higher abundance within the same m/z. The least symmetric are the most unlikely isomers to form and are expected to have the most extended structure and therefore the slowest drift time.

With increasing m/z's from 360 to 536, the width of the distribution first extends with m/z 382 and 426 showing at least seven less resolved structures, and then narrows with fewer distinguishable isomers. The drift time distribution at m/z 492 shows clearly that the more symmetrical distributions are in higher abundance, and the least symmetric structures fade into the background. Because of the larger number of potential isomers, each drift time observed may contain multiple similar-sized extended structures. The cross-section differences of the isomers with smaller m/z values can be expected to be significant, as is observed with the number of detectable drift time distributions, e.g., m/z 360 (six drift time distributions). With increasing size, the statistical likelihood for different structures increases and the relative differences in their cross sections become smaller and therefore more difficult to cleanly separate from each other. Even though the more compact isomers with the shorter drift times are more abundant and resolved at lowest m/z's, beginning at m/z 382, the most symmetrical structure is no longer resolved judging the width of the drift times.

Diagonal slices from the 2-D plot of the doubly charged family were extracted to obtain the mass spectral information at early, middle, and late drift times for each distribution (Figure S3A). The extracted mass spectra have signals at the same m/z, confirming that the drift time distributions of charge state +2 (Figure S3B (**1**) and (**2**)) are isomers or potentially conformers. To differentiate between these principle options, another set of experiments was performed in which ions were drift time selected using the G2 ion gate and activated by applying a potential in IA2 for the purpose of increasing the internal energy of the ions, and where possible, change their conformation,[34−36] which would likely result in a change in drift time after traversing D2 and D3 (Scheme S1). Such activation experiments of the 4-arm branched polymer ions resulted in no change in drift time. These observations indicate that these ions are structural isomers and not conformers.

Contrary to previous results with PEG and other oxygen-rich polymers,[24] no charge-state inversions or sigmoidal transitions were observed in this sample. This absence is an indication of the low number of repeat units per arm that is detectable. In other words, folding transitions are not an option in the short-armed star polymers, contrasted to the same number of polymer monomer units assembled in a linear analogue. The branching of the 4-arm PEG-800 prevents folding transitions related to metal cation charge repulsion and chain rearrangements and are assumed to be related to the presence of the core.

Interestingly, an unexpected singly charged polymer distribution separated by a difference of m/z 44 was detected at shortened drift times relative to those of the doubly charged ions but faster drift times than the singly charged ions of the 4-arm PEG-800 (Figure S3B (**3**)). The presence of a significantly smaller sized PEG-based polymer suggests asymmetric arm growth of the core structure, in which at least one arm did not grow during synthesis. Further studies on what we refer to as a truncated PEG side-product are detailed below.

Blend of 4-Arm Star-Branched PEG-800 and Linear PEG-970. With the observation of a truncated 4-arm polymer, a mixture of linear and 4-arm star polymer was blended for study. The 2-D plot of the polymer blend of a 4-arm star-branched PEG-800 and a linear PEG-970 (Figure 3) resulted in a wide drift time distribution from t_d (m/z) ~19(338) to ~31(624) and t_d (m/z) ~29(582) to ~37(802). The observed drift times are similar to those observed in Figure 1, which correspond to the doubly and singly charged ions of the 4-arm branched polymer (Figure 3A), respectively. Additional doubly charged ions from t_d (m/z) ~24(412) to ~32(610) and singly charged ions from t_d (m/z) ~29(582) to ~37(802) corresponding to linear PEG-970 are also readily detected. The ions of the linear PEG have longer drift times than the star-branched PEG in both the singly charged and the doubly charged ions. These differences must be related to a complete elongation in case of the linear PEG the linear PEG resulting in a more extended structure. Intriguingly, the direct comparison of the doubly charged families reveals that the linear PEG-970 architecture at t_d (m/z) ~25(434) lines up closely to the extended, low-abundant 4-arm architecture, e.g., t_d (m/z) ~24(426). This not only shows that the different architectures can be easily differentiated, but also clarifies that the 4-arm star-branched PEG isomers with longer chain length exhibit longer drift times as they approach an increasingly linear structure. Between these architecturally different polymers, the truncated form of the 4-arm is also detected as singly charged ions. The truncated and the linear polymers, observed as doubly and singly charged ions, are well separated from each other to be directly observed on the IMS-MS 2-D plot without additional extraction procedures of either the drift time or m/z dimensions.

3-Arm Star-Branched PEG-1000. The 3-arm star-branched PEG-1000 sample doped with lithium chloride reveals in the 2-D plot of IMS-MS a family of singly charged ions in the region from t_d (m/z) ~29(580) to ~39(803) with each m/z having

https://dx.doi.org/10.1021/jasms.0c00045
J. Am. Soc. Mass Spectrom. XXXX, XXX, XXX−XXX

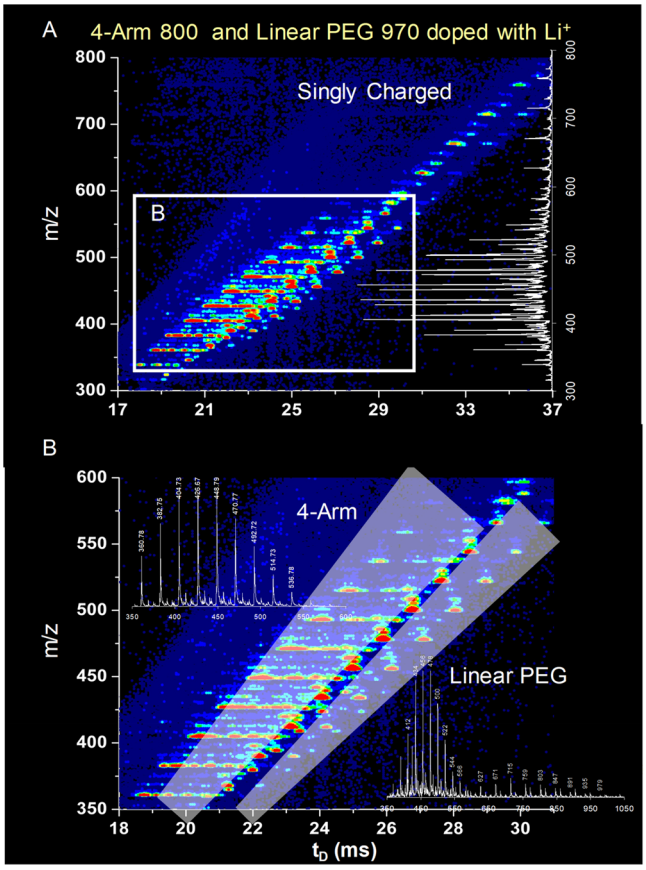

Figure 3. 4-Arm star-branched PEG-800 doped with lithium chloride using home-built IMS-MS. 2-D plot of (A) full range and (B) inset regions. Ion intensities are represented with a false color scale where blue is the lowest intensity, ranging through green to yellow to red, which is the highest intensity.

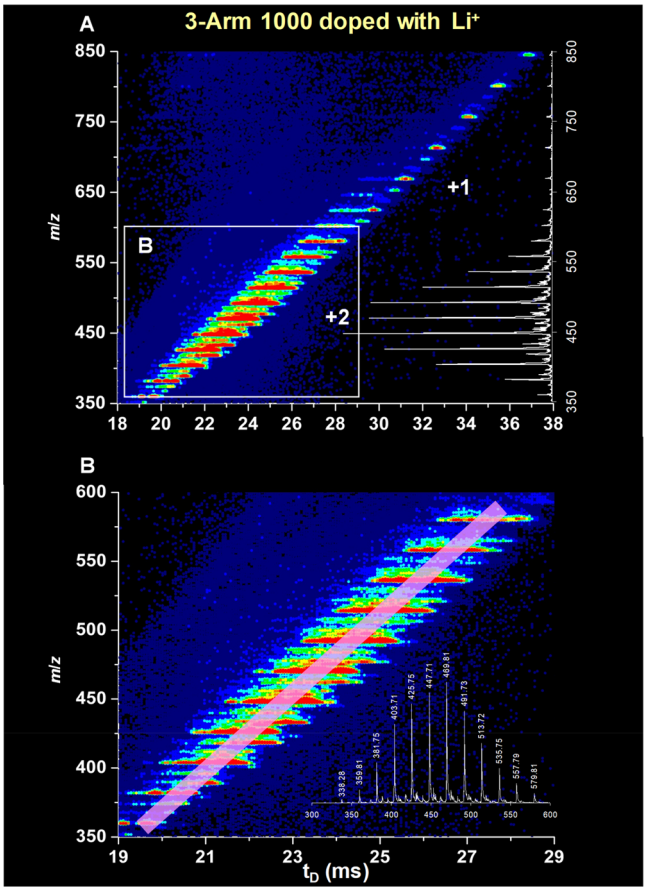

Figure 4. 3-Arm star-branched PEG-1000 doped with lithium chloride using home-built IMS-MS. 2-D plot of (A) full range and (B) inset regions. Ion intensities are represented with a false color scale where blue is the lowest intensity, ranging through green to yellow to red, which is the highest intensity.

associated drift time distributions of a few tenths of a ms for each respective m/z (Figure 4A). A family of doubly charged ions is observed from t_d (m/z) ~19(359) to ~28(579) with associated drift time distributions of roughly 2 ms for each respective m/z (Figure 4A,B). The 3-arm polymer reveals more extended structures, as expected (Scheme 1), relative to that of the 4-arm at ~19(338) to ~26(536) (Figure 2). The drift time distributions of each doubly charged m/z value indicates the presence of many well-resolved drift time distributions (Figure S4). The drift time distributions for the lower m/z's are nearly baseline separated, and with increasing m/z's the drift time distributions show increasing overlaps, similar to the 4-arm sample (Figure 2). These structural isomers are more numerous than those observed in the 4-arm PEG-800 (Figure 2). The extracted drift times of the charge state +1 show no separation of isomers charged only by one cation (Figure S5), as was the case with the 4-arm polymer (Figure S2).

A direct comparison of the drift time distributions summed over all the m/z values where polymer ions were observed for the 3-arm and 4-arm star-branched architectures is shown in Figure 5. The overall distributions of the 3-arm polymer (Figure 5A) are observed with shortened drift times relative to the 4-arm polymer (Figure 5B). The 2+ charge is centered for the 3-arm polymer at ca. 25.5 ms versus the 4-arm polymer ca. 23 ms. This is a result of the 3-arm polymer likely having the statistically longer and more extended arms as well as the presence of a slightly higher MW (PEG-1000 versus PEG-800), which

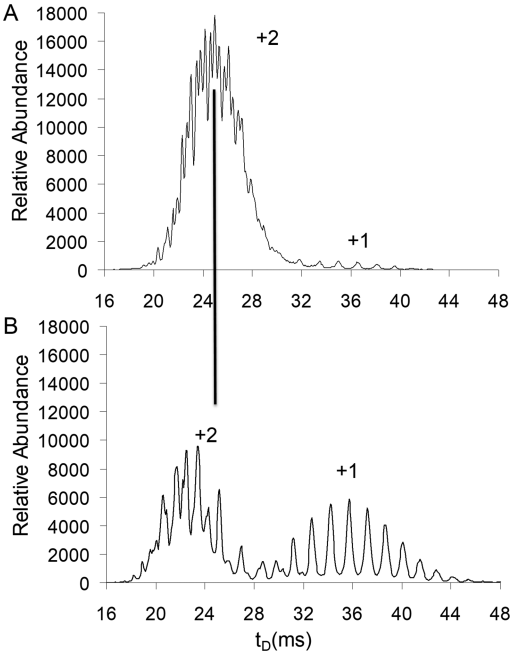

Figure 5. Direct comparison of the drift time distributions summed over all the m/z values where polymer ions were observed for the (A) 3-arm and (B) 4-arm star-branched PEG polymer.

https://dx.doi.org/10.1021/jasms.0c00045
J. Am. Soc. Mass Spectrom. XXXX, XXX, XXX−XXX

lengthens the total of the arms by an average of 4.5 monomer units. Further, the intensity ratio of doubly relative to singly charged ions in the total drift time distribution of the 3-arm PEG-1000 polymer is greater than that observed in the 4-arm PEG-800 polymer. The significantly higher ratio of doubly to singly charged ions is another signature of longer arm length in the 3-arm star-branched polymer compared to that of the 4-arm. High resolution measurements using a commercial high resolution mass spectrometer (Figure S1) also shows differences in charge state distributions for these two samples. These observations support the suggested depictions in Scheme 2.

The elongated 3-arm polymer can form asymmetric arms by the addition of only a few monomer units altering the structure from the symmetric to asymmetric (Scheme 1B). The asymmetric 3-arm molecules are intrinsically related to longer molecules with extended gas-phase ion structures resulting in smaller differences in shapes. These less resolved structures require an increase in IMS resolving power to separate such structures.

4-Arm Star-branched PEG-2000. The 2-D plot of IMS-MS for the 4-arm star-branched PEG-2000 sample doped with lithium chloride has a different appearance to similar plots for the smaller star-branched polymers (Figure 6). Depicting a more precise t_d (m/z) range is challenging for the different charge state distributions because of the various charge state families present causing overlap in both the drift time and m/z dimensions. The m/z extraction of each charge-state shows a range of charges (1−3) (Figure 6B). Interestingly, the triply charged ions fall in the general region of t_d (m/z) ~28(550) to ~34(750) between the +1 and +2 charges. Besides the intense multiply charged ions, singly charged low-molecular weight ions of $[PEG + Li]^+$ were also detected at ca. m/z 500 to 750 (Figure S6), showing a similar pattern observed in the 4-arm PEG-800 of an unreacted or truncated PEG-based impurity. In the m/z dimension, these ions are not identified or go unnoticed (Figure S1B). We hypothesis that with increasing size of the star-branched polymers, the 2-D plots of IMS-MS become increasingly more complicated, but in the pictorials the structural diversity of the sample is immediately apparent.

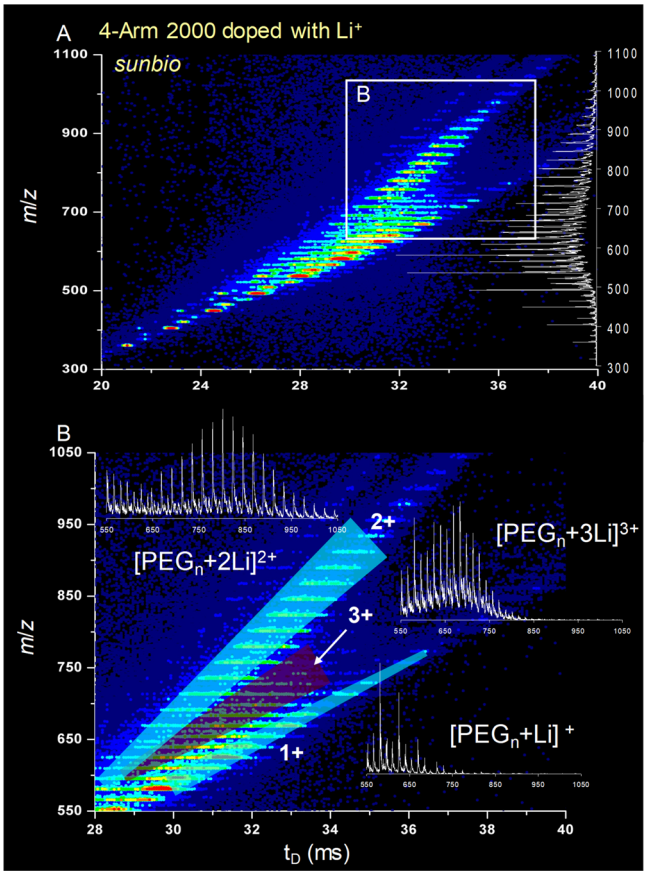

Figure 6. ESI-IMS-MS of 4-arm PEG 2000 doped with LiCl displayed as a 2-D plot of drift time versus m/z. (A) Full range with inset of total mass spectrum and (B) inset region with three extracted mass spectral regions of charge states +1 to +3.

The extraction of specific m/z values for the different charge states of 3-arm branched PEG-1000 reveal different drift time distributions (Figure S7) indicating that isomers have been (partially) resolved. These isomers cover a range of ca. 3 ms for charge state +1, ca. 6 ms for charge state +2, and at least 8 ms for charge state +3 in the drift time dimension. Although there is notable overlap of charge states in the 2D plot, the increase in width of the distribution of +2 relative to +1 suggests an increasing number of gas-phase structures. Further improvements in ion mobility resolution may more effectively resolve these ever complex samples.

Commercial IMS-MS: Different Ionization Methods, Salts, and Robustness through Source Modifications. Similar experiments have been performed using a TWIMS (Waters SYNAPT G2) comparing various ionization methods that are known to form multiply charged ions (ESI, *v*MAI, and LSI) and singly charged ions (MALDI), respectively. Various metal salts were explored as ionization agents, as one must expect differences in ionization depending on the salts added during sample preparation.[20−27,31,44−48] Detailed information can be found in the Supporting Information.

ESI for the analysis of the pure branched and linear polymers was first employed, showing similar trends observed with the home-built instrument using LiCl. Preliminary ESI-IMS-MS and MS/MS analyses of the 4-arm branched PEG (MW 800) are included in the Supporting Information (Figure S8). The binary mixture of 4-arm branched and the linear PEG using the dopant LiCl is seen in Figure S9. From the 2D plot, similar +1 and +2 charge states were detected as observed with the home-built instrument (Figure 1A), and the extracted m/z's for charge states +1 and +2 are provided in Figure S10. By extracting the drift time for a specific ion, e.g., m/z 427.2 (+2), the separation of gas-phase isomers is observed (Figure S9). While the drift time resolution is not nearly as apparent as on the home-built instrument (Figure 2), similar features in the drift time distributions are observed (Figure S9A). Importantly, a similar 2-D plot (Figure S9B) is obtained for the 4-arm branched polymer and linear PEG, as observed on the home-built instrument (Figure 3).

Performing similar experiments utilizing *v*MAI-IMS-MS on the SYNAPT G2 for the pure (3-arm branched PEG-1000 and linear PEG-DME-2000) and binary mixture of the branched polymer sample (3-arm branched PEG-1000 and 4-arm branched PEG-800) resulted in similar trends as those obtained with home-built ESI-IMS-MS. However, these results were achieved directly from surfaces (Figure S11). The pictorials are notably different and the extracted drift times provide an indication of the different architectures for the specific m/z values. This differentiation is not obvious using a MS approach alone (Figure S1 and S11B (1)).

https://dx.doi.org/10.1021/jasms.0c00045
J. Am. Soc. Mass Spectrom. XXXX, XXX, XXX−XXX

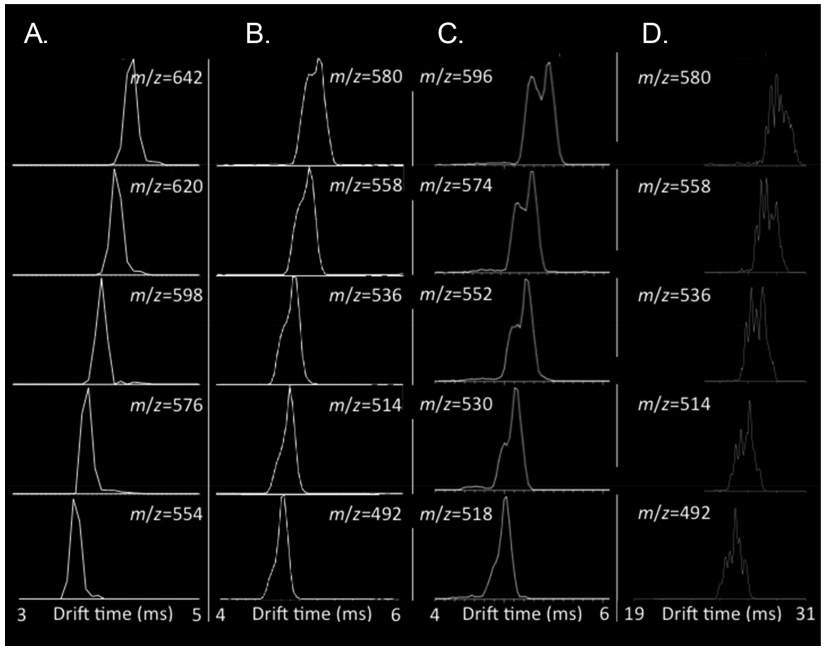

Figure 7. Extracted drift times for 3-arm branched PEG 1000 using *v*MAI on a commercial IMS-MS instrument (SYNAPT G2) doped with cationization agents of (A) $Ba(Ac_2)$, (B) LiTFA, and (C) NaTFA. (D) Comparison with the extracted drift times of 3-arm branched PEG 1000 doped with LiCl acquired on a home-built 3-m ESI-IMS-MS instrument.

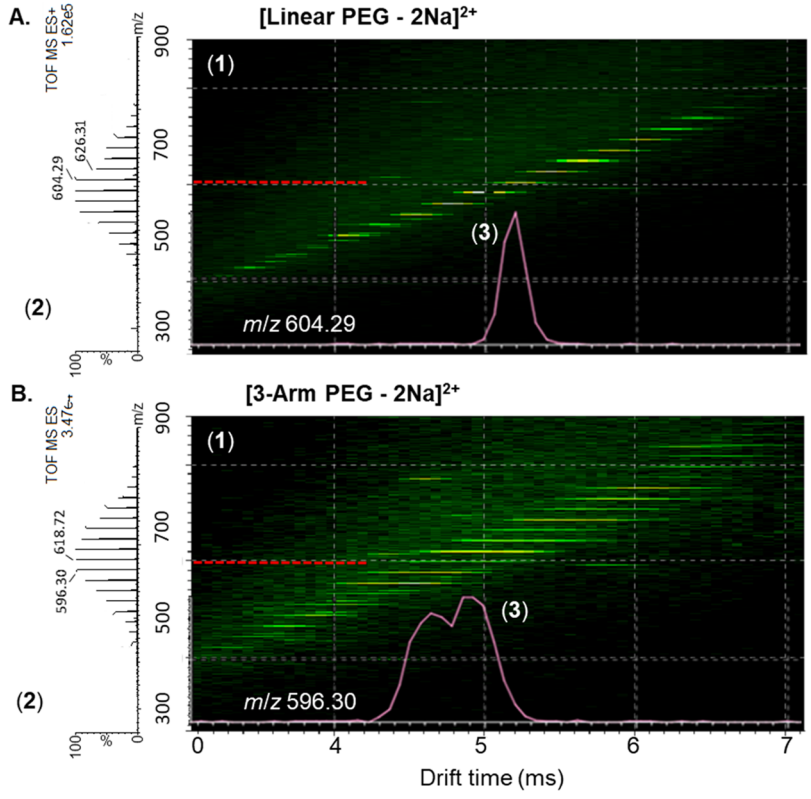

Figure 8. vMAI-IMS-MS of (A) linear PEG-1000 and (B) 3-arm PEG-1000 doped with sodium trifluoroacetate: (1) 2-D plot of drift time over *m*/*z*; (2) total mass spectrum; (3) extracted drift times. Ion intensities are represented with a false color scale where blue is the lowest intensity, ranging through green to yellow to red, which is the highest intensity. The MS™ prototype vacuum-probe source,[69] which replaces the ESI source, was used for robust, prompt ionization. A manual sample introduction platform guides a probe device directly into the inlet aperture to expose matrix/analyte sample on the tip of the probe directly to the vacuum of the mass spectrometer (SYNAPT G2S) without physical contact with source elements. The ionization occurs spontaneous. A molar ratio of matrix (3-NBN)/analyte (25 pmol)/salt (1:1:50) was used by spotting equal volumes of the respective solutions on the probe and followed by brief drying.

https://dx.doi.org/10.1021/jasms.0c00045
J. Am. Soc. Mass Spectrom. XXXX, XXX, XXX−XXX

Comparing the 2-D plots for the same matrix/analyte/salt ratio using either *v*MAI (Figure S12A) or ESI (Figure S12B) on the same commercial IMS-MS instrument shows a difference in observed ion abundances. In addition to the metal cation adducted doubly charged ions, the *v*MAI results show the presence of doubly charged ions consistent with protonation, which are present at lower abundance in the ESI results.

Typically, monovalent cations using various different salts associate with polymers.[20−27,31,44−48] In our IMS-MS study here we expand to different cations including also divalent cations and study the effect on the drift time separation. Both the divalent versus two monovalent cations provided the doubly charged ions to the oligomer, which is likely a matter of the size of the oligomer. Each cation is expected to be surrounded by oxygen giving rise to multiple coordination's of oxygens (number of repeat units of the oligomer) relative to a cation(s) size and, likely, charge state. Two charges at the same position, as is the case with Ba^{2+}, should not result in extending the polymer structure through charge repulsion as is the case with the hypothesis outlined in Scheme 2 for two monovalent ions solvated from each other by the oxygen-rich PEG. This could explain the relatively poor drift time separation of the divalent cation (Figure 7A), as compared to two charges separable from each other in the case of monovalent cations (Figure 7B,C). This is in agreement with the hypothesis that the repulsive forces of two charges are necessary for elongating the gas-phase structure and effectively separating and detecting them by IMS-MS. Alternatively, but unlikely, the results may indicate the possibility of preferential isomer selection of the branched PEG ions using Ba^{2+} for which very little is known in the literature. Differentiating between the two possibilities will require further studies. To the best of our knowledge, this interesting observation of the differences in IMS separation based on divalent and monovalent cations with the same number of charges noncovalently attached to an oligomer/polymer has not been described in the literature.

Changing the size of the monovalent cation as metal salt additions improved the separation of the isomeric branched polymer ions using MAI-IMS-MS, resulting in better resolved drift times (Figure 7). This improved drift time resolution is observed for the doubly charged ions $[M + 2Na]^{2+}$ (Figure 7C) as compared to $[M + 2Li]^{2+}$ (Figure 7B). The ESI-IMS-MS measurements on the home-built instrument using LiCl is shown for comparison purposes (Figure 7D). As long as multiply charged ions are formed, the 3-arm branched PEG-1000 ions, also relative to linear PEG-1000, are significantly better resolved than the singly charged ions formed by MALDI using the same mass spectrometer (Figure S13). The extracted charge states using the MAI-IMS-MS approach are displayed in Figure S14 and preliminary LSI-ETD results in Figure S15. The success and advantages associated with formation of multiply charged polymer ions is in agreement with early studies on desolvation relative to the size of the cation and the length of the oligomers.[23−25,31]

In a final set of experiments, a prototype MAI vacuum-probe[69] was used on the Waters SYNAPT G2S to analyze linear PEG-970 (Figure 8A) and 3-arm branched PEG-1000 (Figure 8B). As expected, the mass spectra of these oligomers with similar MWs does not differentiate the structural differences. Importantly, the 2-D IMS-MS pictorials appear closely related to those previously observed with ESI on the SYNAPT G2 and home-built IMS-MS instruments. The extraction of m/z 604.29 for the linear PEG (Figure 8A (**3**)) shows the typical relatively narrow distribution similar to the results obtained with ESI (Figure 3). Notably, the extraction of m/z 596.30 for the 3-arm branched PEG-1000 (Figure 8B (**3**)) reveals the much broader drift time distributions, which are indicative of the presence of more structural features. The *v*MAI probe relative to ESI eliminates capillary clogging and source contamination, improves IMS-MS resolution, and allows direct detection of materials from surfaces.

CONCLUSION

The successful differentiation of isomeric architectural variation is achieved simply and rapidly based on the different cross sections (size, shape, and charge) of the gaseous multiply charged ions using an IMS-MS instrument. The high drift time resolution provides insight into complex isomeric structures not readily obtainable with other technologies. Importantly, the observation that isomers with shorter drift times have higher ion abundance than isomers with longer drift times elegantly discloses that asymmetric, and thus more linear, isomers were less likely formed during synthesis. The unique 2-D plots of IMS-MS for the polymers examined provides a pictorial that can potentially be used for quality control monitoring. For example, the sample characterization demonstrated the presence of low abundant impurities, best described as truncated 3-arm in the 4-arm star-polymer. While the home-built IMS-MS instrument provides higher IMS drift time resolution, it was demonstrated that the commercial TWIMS instrument can rapidly differentiate the star branched polymers. Furthermore, the MAI allows direct analysis from surfaces generating the necessary multiply charged ions for effective IMS-MS separation with improved drift time resolution.[70−72] Future efforts will be focused on incorporating recognition software assisting in the analysis of the 2-D plots for rapid characterization and quality control purposes.

ASSOCIATED CONTENT

Supporting Information

The Supporting Information is available free of charge at https://pubs.acs.org/doi/10.1021/jasms.0c00045.

Schematic of the IMS-IMS-IMS-TOF instrument. Figures of Orbitrap high-resolution MS; extracted drift time distributions; 2D plots; commercial ESI-IMS-MS; vMAI-IMS-MS; vMAI and MALDI; LSI of 3-arm branched PEG-1000 (PDF)

AUTHOR INFORMATION

Corresponding Author

Barbara S. Larsen − *DuPont, Nutrition & Biosciences, Wilmington, Delaware 19808, United States*; Email: barbara.s.larsen@dupont.com

Authors

Calvin A. Austin − *Department of Chemistry, Wayne State University, Detroit, Michigan 48202, United States*; orcid.org/0000-0001-6094-0078

Ellen D. Inutan − *Department of Chemistry, Wayne State University, Detroit, Michigan 48202, United States*

Brian C. Bohrer − *Department of Chemistry, Indiana University, Bloomington, Indiana 47405, United States*

Jing Li − *Department of Chemistry, Wayne State University, Detroit, Michigan 48202, United States*

https://dx.doi.org/10.1021/jasms.0c00045
J. Am. Soc. Mass Spectrom. XXXX, XXX, XXX−XXX

Joshua L. Fischer − *Department of Chemistry, Wayne State University, Detroit, Michigan 48202, United States;* orcid.org/0000-0001-6183-8606
Kanchana Wijerathne − *Department of Chemistry, Wayne State University, Detroit, Michigan 48202, United States*
Casey D. Foley − *Department of Chemistry, Wayne State University, Detroit, Michigan 48202, United States*
Christopher B. Lietz − *Department of Chemistry, Wayne State University, Detroit, Michigan 48202, United States*
Daniel W. Woodall − *Department of Chemistry, Wayne State University, Detroit, Michigan 48202, United States*
Lorelie F. Imperial − *Department of Chemistry, Wayne State University, Detroit, Michigan 48202, United States*
David E. Clemmer − *Department of Chemistry, Indiana University, Bloomington, Indiana 47405, United States;* orcid.org/0000-0003-4039-1360
Sarah Trimpin − *Department of Chemistry, Wayne State University, Detroit, Michigan 48202, United States;* orcid.org/0000-0002-3720-2269

Complete contact information is available at: https://pubs.acs.org/10.1021/jasms.0c00045

Notes

The authors declare no competing financial interest.

■ ACKNOWLEDGMENTS

The authors are grateful for the financial support from NSF CHE-1411376 (to S.T.) and NSF SBIR Phase I (to MS^{TM}), DuPont Young Professor Award (to S.T.), Wayne State University (WSU) Undergraduate Research Opportunities Program (to J.L.F.), Rumble Fellowship (to C.D.F and E.D.I.), Initiative for Maximizing Student Diversity Fellowship (to C.A.A.), Schaap Graduate Fellowship (to E.D.I.), Schaap Faculty Scholar Award (to S.T.), and Waters Center of Innovation Program (to S.T. and D.E.C). Any opinions, findings, and conclusions or recommendations expressed in this material are those of the authors and do not necessarily reflect the views of the National Science Foundation.

■ REFERENCES

(1) Kadam, P. G.; Mhaske, S. Synthesis of Star-Shaped Polymers. *Des. Monomers Polym.* **2011**, *14*, 515−540.
(2) Inoue, K. Functional Dendrimers, Hyperbranched and Star Polymers. *Prog. Polym. Sci.* **2000**, *25*, 453−571.
(3) Daoud, M.; Cotton, J. Star Shaped Polymers: A Model for the Conformation and its Concentration Dependence. *J. Phys. (Paris)* **1982**, *43*, 531−538.
(4) Hedrick, J. L.; Trollsas, M.; Hawker, C. J.; Atthoff, B.; Claesson, H.; Heise, A.; Miller, R. D.; Mecerreyes, D.; Jerome, R.; Dubois, P. Dendrimer-like Star Block and Amphiphilic Copolymers by Combination of Ring Opening and Atom Transfer Radical Polymerization. *Macromolecules* **1998**, *31*, 8691−8705.
(5) Cloutet, E.; Fillaut, J. L.; Astruc, D.; Gnanou, Y. Newly Designed Star-shaped Polystyrene: Synthesis and Characterization. *Macromolecules* **1998**, *31*, 6748−6755.
(6) Cai, Q.; Zhao, Y.; Bei, J.; Xi, F.; Wang, S. Synthesis and Properties of Star-shaped Polylactide Attached to Poly(amidoamine) Dendrimer. *Biomacromolecules* **2003**, *4*, 828−834.
(7) Knischka, R.; Lutz, P. J.; Sunder, A.; Mülhaupt, R.; Frey, H. Functional Poly(ethylene oxide) Multiarm Star Polymers: Core-first Synthesis using Hyperbranched Polyglycerol Initiators. *Macromolecules* **2000**, *33*, 315−320.
(8) Lapienis, G. Star-shaped Polymers having PEO arms. *Prog. Polym. Sci.* **2009**, *34*, 852−892.
(9) Hadjichristidis, N.; Pitsikalis, M.; Pispas, S.; Iatrou, H. Polymers with Complex Architecture by Living Anionic Polymerization. *Chem. Rev.* **2001**, *101*, 3747−3792.
(10) Myers, B. K.; Zhang, B.; Lapucha, J. E.; Grayson, S. M. The Characterization of Dendronized Poly(ethylene glycol)s and Poly(ethylene glycol) Multi-arm Stars using Matrix-assisted Laser Desorption/Ionization Time-of-Flight Mass Spectrometry. *Anal. Chim. Acta* **2014**, *808*, 175−189.
(11) Trimpin, S.; Weidner, S. M.; Falkenhagen, J.; McEwen, C. N. Fractionation and Solvent-free MALDI-MS Analysis of Polymers using Liquid Adsorption Chromatography at Critical Conditions in Combination with a Multisample On-target Homogenization/Transfer Sample Preparation Method. *Anal. Chem.* **2007**, *79*, 7565−7570.
(12) Girod, M.; Phan, T. N. T.; Charles, L. On-line Coupling of Liquid Chromatography at Critical Conditions with Electrospray Ionization Tandem Mass Spectrometry for the Characterization of a Nitroxide-mediated Poly(ethylene oxide)/Polystyrene Block Copolymer. *Rapid Commun. Mass Spectrom.* **2008**, *22*, 3767−3775.
(13) Weidner, S. M.; Falkenhagen, J.; Bressler, I. Copolymer Composition Determined by LC-MALDI-TOF MS Coupling and "MassChrom2D" Data Analysis. *Macromol. Chem. Phys.* **2012**, *213*, 2404−2411.
(14) Barner-Kowollik, C.; Till Gründling, T.; Falkenhagen, J.; Weidner, S. *Mass Spectrometry in Polymer Chemistry*; Wiley-VCH, 2012.
(15) Schoenmakers, P.; Aarnoutse, P. Multi-dimensional Separations of Polymers Synthetic Polymers and Comprehensive Two-dimensional Liquid Chromatography (LC × LC) are a Synergistic Combination. LC × LC Provides Unique Insights in Mutually Dependent Molecular Distributions. Synthetic Polymers Offer Clear Demonstrations of the Value of LC × LC. *Anal. Chem.* **2014**, *86*, 6172−6179.
(16) Epping, R.; Panne, U.; Falkenhagen, J. Power of Ultra Performance Liquid Chromatography/Electrospray Ionization-MS Reconstructed Ion Chromatograms in the Characterization of Small Differences in Polymer Microstructure. *Anal. Chem.* **2018**, *90* (5), 3467−3474.
(17) Wesdemiotis, C. Multidimensional Mass Spectrometry of Synthetic Polymers and Advanced Materials. *Angew. Chem., Int. Ed.* **2017**, *56*, 1452−1464.
(18) de Koster, C. G.; Duursma, M. C.; van Rooij, G. J.; Heeren, R. M. A.; Boon, J. J. Endgroup Analysis of Polyethylene Glycol Polymers by Matrix-assisted Laser Desorption/ionization Fourier-Transform Ion Cyclotron Resonance Mass Spectrometry. *Rapid Commun. Mass Spectrom.* **1995**, *9*, 957−962.
(19) Crotty, S.; Gerislioglu, S.; Endres, K. J.; Wesdemiotis, C.; Schubert, U. S. Polymer Architectures via Mass Spectrometry and Hyphenated Techniques: A review. *Anal. Chim. Acta* **2016**, *932*, 1−21.
(20) Przybilla, L.; Francke, V.; Räder, H. J.; Müllen, K. Block Length Determination of a Poly(ethylene oxide)-b-poly(p-phenylene ethynylene) Diblock Copolymer by Means of MALDI-TOF Mass Spectrometry Combined with Fragment-Ion Analysis. *Macromolecules* **2001**, *34*, 4401−4405.
(21) Wyttenbach, T.; von Helden, G.; Bowers, M. T. Conformations of Alkali Ion Cationized Polyethers in the Gas Phase: Polyethylene Glycol and Bis [(benzo-15-crown-5)-15-ylmethyl] pimelate. *Int. J. Mass Spectrom. Ion Processes* **1997**, *165-166*, 377−390.
(22) Gidden, J.; Wyttenbach, T.; Jackson, A. T.; Scrivens, J. H.; Bowers, M. T. Gas-Phase Conformations of Synthetic Polymers: Poly(ethylene glycol), Poly(propylene glycol), and Poly(tetramethylene glycol). *J. Am. Chem. Soc.* **2000**, *122*, 4692−4699.
(23) Trimpin, S.; Plasencia, M.; Isailovic, D.; Clemmer, D. E. Resolving Oligomers from Fully Grown Polymers with IMS-MS. *Anal. Chem.* **2007**, *79*, 7965−7974.
(24) Trimpin, S.; Clemmer, D. E. Ion Mobility Spectrometry/Mass Spectrometry Snapshots for Assessing the Molecular Compositions of Complex Polymeric Systems. *Anal. Chem.* **2008**, *80*, 9073−9083.
(25) Larriba, C.; de la Mora, J. F.; Clemmer, D. E. Electrospray Ionization Mechanisms for Large Polyethylene Glycol Chains Studied Through Tandem Ion Mobility Spectrometry. *J. Am. Soc. Mass Spectrom.* **2014**, *25*, 1332−1345.

(26) Wilkins, C. L.; Trimpin, S. *Ion Mobility Spectrometry: Theory and Applications*; Taylor and Francis Group, 2010.
(27) Crotty, S.; Gerislioglu, S.; Endres, K. J.; Wesdemiotis, C.; Schubert, U. S. Polymer Architectures via Mass Spectrometry and Hyphenated Techniques: A review. *Anal. Chim. Acta* **2016**, *932*, 1−21.
(28) Hoaglund, C. S.; Valentine, S. J.; Sporleder, C. R.; Reilly, J. P.; Clemmer, D. E. Three-Dimensional Ion Mobility/TOFMS Analysis of Electrosprayed Biomolecules. *Anal. Chem.* **1998**, *70*, 2236−2242.
(29) Henderson, S. C.; Valentine, S. J.; Counterman, A. E.; Clemmer, D. E. ESI/Ion Trap/Ion Mobility/Time-of-Flight Mass Spectrometry for Rapid and Sensitive Analysis of Biomolecular Mixture. *Anal. Chem.* **1999**, *71*, 291−301.
(30) Alexander, N. E.; Swanson, J. P.; Joy, A.; Wesdemiotis, C. Sequence Analysis of Cyclic Polyester Copolymers using Ion Mobility Tandem Mass Spectrometry. *Int. J. Mass Spectrom.* **2018**, *429*, 151−157.
(31) Gidden, J.; Wyttenbach, T.; Batka, J. J.; Weis, P.; Jackson, A. T.; Scrivens, J. H.; Bowers, M. T. Folding Energetics and Dynamics of Macromolecules in the Gas Phase: Alkali Ion-Cationized Poly(ethylene terephthalate) Oligomers. *J. Am. Chem. Soc.* **1999**, *121*, 1421−1422.
(32) Chen, L.; Shao, Q.; Gao, Y. Q.; Russell, D. H. Molecular Dynamics and Ion Mobility Spectrometry Study of Model β-Hairpin Peptide, Trpzip1. *J. Phys. Chem. A* **2011**, *115*, 4427−4435.
(33) Bohrer, B. C.; Clemmer, D. E. Biologically-inspired Peptide Reagents for Enhancing IMS-MS Analysis of Carbohydrates. *J. Am. Soc. Mass Spectrom.* **2011**, *22*, 1602−1609.
(34) Koeniger, S. L.; Merenbloom, S. I.; Valentine, S. J.; Jarrold, M. F.; Udseth, R. D.; Smith, R. D.; Clemmer, D. E. An IMS−IMS Analogue of MS−MS. *Anal. Chem.* **2006**, *78*, 4161−4174.
(35) Koeniger, S. L.; Clemmer, D. E. Resolution and Structural Transitions of Elongated States of Ubiquitin. *J. Am. Soc. Mass Spectrom.* **2007**, *18*, 322−331.
(36) Koeniger, S. L.; Merenbloom, S. I.; Sevugarajan, S.; Clemmer, D. E. Transfer of Structural Elements from Compact to Extended States in Unsolvated Ubiquitin. *J. Am. Chem. Soc.* **2006**, *128*, 11713−11719.
(37) Duez, Q.; Chirot, F.; Liénard, R.; Josse, T.; Choi, C.; Coulembier, O.; Dugourd, P.; Cornil, J.; Gerbaux, P.; De Winter, J. Polymers for Traveling Wave Ion Mobility Spectrometry Calibration. *J. Am. Soc. Mass Spectrom.* **2017**, *28*, 2483−2491.
(38) Duez, Q.; Metwally, H.; Konermann, L. Electrospray Ionization of Polypropylene glycol: Rayleigh-Charged Droplets, Competing Pathways, and Charge State-dependent Conformations. *Anal. Chem.* **2018**, *90*, 9912−9920.
(39) Kokubo, S.; Vana, P. Obtaining the Dielectric Constant of Polymers from Doubly Charged Species in Ion-mobility Mass Spectrometry. *Macromol. Chem. Phys.* **2017**, *218*, 1700126.
(40) Kanu, A. B.; Dwivedi, P.; Tam, M.; Matz, L.; Hill, H. H., Jr. Ion Mobility−Mass Spectrometry. *J. Mass Spectrom.* **2008**, *43*, 1−22.
(41) Bohrer, B. C.; Merenbloom, S. I.; Koeniger, S. L.; Hilderbrand, A. E.; Clemmer, D. E. Biomolecule Analysis by Ion Mobility Spectrometry. *Annu. Rev. Anal. Chem.* **2008**, *1*, 293−327.
(42) Ewing, M. A.; Glover, M. S.; Clemmer, D. E. Hybrid Ion Mobility and Mass Spectrometry as a Separation Tool. *J. Chrom. A* **2016**, *1439*, 3−25.
(43) May, J. C.; McLean, J. A. Ion Mobility-Mass Spectrometry: Time-dispersive Instrumentation. *Anal. Chem.* **2015**, *87*, 1422−1436.
(44) Hoskins, J. N.; Trimpin, S.; Grayson, S. M. Architectural Differentiation of Linear and Cyclic Polymeric Isomers by Ion Mobility Spectrometry-Mass Spectrometry. *Macromolecules* **2011**, *44*, 6915−6918.
(45) Morsa, D.; Defize, T.; Dehareng, D.; Jérôme, C.; De Pauw, E. Polymer Topology Revealed by Ion Mobility Coupled with Mass Spectrometry. *Anal. Chem.* **2014**, *86*, 9693−9700.
(46) Zhang, W.; Quernheim, M.; Räder, H. J.; Müllen, K. Collision-induced Dissociation Ion Mobility Mass Spectrometry for the Elucidation of Unknown Structures in Strained Polycyclic Aromatic Hydrocarbon Macrocycles. *Anal. Chem.* **2016**, *88*, 952−959.
(47) Alexander, N. E.; Swanson, J. P.; Joy, A.; Wesdemiotis, C. Sequence Analysis of Cyclic Polyester Copolymers using Ion Mobility Tandem Mass Spectrometry. *Int. J. Mass Spectrom.* **2018**, *429*, 151−157.
(48) Foley, C. D.; Zhang, B.; Alb, A. M.; Trimpin, S.; Grayson, S. M. The Use of Ion Mobility Spectrometry-Mass Spectrometry to Elucidate Arm-dispersity within Star Polymers. *ACS Macro Lett.* **2015**, *4*, 778−782.
(49) Whitehouse, C. M.; Dreyer, R. N.; Yamashita, M.; Fenn, J. B. Electrospray Interface for Liquid Chromatographs and Mass Spectrometers. *Anal. Chem.* **1985**, *57*, 675−679.
(50) Fenn, J. B.; Mann, M.; Meng, C. K.; Wong, S. F.; Whitehouse, C. M. Electrospray Ionization for Analysis of Large Molecules. *Science* **1989**, *246*, 64−67.
(51) Tanaka, K.; Waki, H.; Ido, Y.; Akita, S.; Yoshida, Y.; Yoshida, T.; Matsuo, T. Protein and Polymer Analysis up to m/z 100,000 by Laser Ionization Time-of-Flight Mass Spectrometry. *Rapid Commun. Mass Spectrom.* **1988**, *2*, 151−153.
(52) Karas, M.; Hillenkamp, F. Laser Desorption Ionization of Proteins with Molecular Masses Exceeding 10,000 Da. *Anal. Chem.* **1988**, *60*, 2299−2301.
(53) McEwen, C. N.; McKay, R. G.; Larsen, B. S. Analysis of Solids, Liquids, and Biological Tissues using Solid Probe Introduction at Atmospheric Pressure on Commercial LC/MS Instruments. *Anal. Chem.* **2005**, *77*, 7826−7831.
(54) Mendes Siqueira, A. L.; Beaumesnil, M.; Hubert-Roux, M.; Loutelier-Bourhis, C.; Afonso, C.; Bai, Y.; Courtiade, M.; Racaud, A. Atmospheric Solid Analysis Probe Coupled to Ion Mobility Spectrometry-Mass Spectrometry, a Fast and Simple Method for Polyalphaolefin Characterization. *J. Am. Soc. Mass Spectrom.* **2018**, *29*, 1678−1687.
(55) Vieillard, J.; Hubert-Roux, M.; Brisset, F.; Soulignac, C.; Fioresi, F.; Mofaddel, N.; Morin-Grognet, S.; Afonso, C.; Le Derf, F. Atmospheric Solid Analysis Probe-Ion Mobility Mass Spectrometry: An Original Approach to Characterize Grafting on Cyclic Olefin Copolymer Surfaces. *Langmuir* **2015**, *31*, 13138−13144.
(56) Fischer, J. L.; Lutomski, C. A.; El-Baba, T. J.; Siriwardena-Mahanama, B. N.; Weidner, S. M.; Falkenhagen, J.; Allen, M. J.; Trimpin, S. Matrix-assisted Ionization-Ion Mobility Spectrometry-Mass Spectrometry: Selective Analysis of a Europium-PEG Complex in a Crude Mixture. *J. Am. Soc. Mass Spectrom.* **2015**, *26*, 2086−2095.
(57) Trimpin, S.; Lutomski, C. A.; El-Baba, T. J.; Woodall, D. W.; Foley, C. D.; Manly, C. D.; Wang, B.; Liu, C. W.; Harless, B. M.; Kumar, R.; Imperial, L. F.; Inutan, E. D. Magic Matrices for Ionization in Mass Spectrometry. *Int. J. Mass Spectrom.* **2015**, *377* (SI), 532−545.
(58) Trimpin, S.; Inutan, E. D.; Herath, T. N.; McEwen, C. N. Matrix-assisted Laser Desorption/Ionization Mass Spectrometry Method for Selectively Producing Either Singly or Multiply Charged Molecular Ions. *Anal. Chem.* **2010**, *82*, 11−15.
(59) Trimpin, S.; Inutan, E. D. Matrix Assisted Ionization in Vacuum, a Sensitive and Widely Applicable Ionization Method for Mass Spectrometry. *J. Am. Soc. Mass Spectrom.* **2013**, *24*, 722−732.
(60) McEwen, C. N.; Larsen, B. S.; Trimpin, S. Laserspray Ionization on a Commercial Atmospheric Pressure-MALDI Mass Spectrometer Ion Source: Selecting Singly or Multiply Charged Ions. *Anal. Chem.* **2010**, *82*, 4998−5001.
(61) Trimpin, S.; Wang, B.; Inutan, E. D.; Li, J.; Lietz, C. B.; Harron, A.; Pagnotti, V. S.; Sardelis, D.; McEwen, C. N. A Mechanism for Ionization of Nonvolatile Compounds in Mass Spectrometry: Considerations from MALDI and Inlet Ionization. *J. Am. Soc. Mass Spectrom.* **2012**, *23*, 1644−1660.
(62) Trimpin, S. "Magic" Ionization Mass Spectrometry. *J. Am. Soc. Mass Spectrom.* **2016**, *27*, 4−21.
(63) Trimpin, S. Novel Ionization Processes for Use in Mass Spectrometry: 'Squeezing' Nonvolatile Analyte Ions from Crystals and Droplets. *Rapid Commun. Mass Spectrom.* **2019**, *33* (SI), 96−120.
(64) Trimpin, S.; Inutan, E. D.; Karki, S.; Elia, E. A.; Zhang, W. J.; Weidner, S. M.; Marshall, D. D.; Hoang, K.; Lee, C.; Davis, E. T. J.; Smith, V.; Meher, A. K.; Cornejo, M.; Auner, G. W.; McEwen, C. N. Fundamental Studies of New Ionization Technologies and Insights from IMS-MS. *J. Am. Soc. Mass Spectrom.* **2019**, *30*, 1133−1147.

https://dx.doi.org/10.1021/jasms.0c00045
J. Am. Soc. Mass Spectrom. XXXX, XXX, XXX−XXX

(65) El-Baba, T. J.; Lutomski, C. A.; Wang, B.; Trimpin, S. Characterizing Synthetic Polymers and Additives using New Ionization Methods for Mass Spectrometry. *Rapid Commun. Mass Spectrom.* **2014**, *28*, 1175−1184.
(66) Pierson, N. A.; Chen, L.; Valentine, S. J.; Russell, D. H.; Clemmer, D. E. Number of Solution States of Bradykinin from Ion Mobility and Mass Spectrometry Measurements. *J. Am. Chem. Soc.* **2011**, *133*, 13810−13813.
(67) Merenbloom, S. I.; Koeniger, S. L.; Valentine, S. J.; Plasencia, M. D.; Clemmer, D. E. IMS−IMS and IMS−IMS−IMS/MS for Separating Peptide and Protein Fragment Ions. *Anal. Chem.* **2006**, *78*, 2802−2809.
(68) Inutan, E. D.; Meher, A. K.; Karki, S.; Fischer, J. L.; Imperial, L. F.; Foley, C. D.; Jarois, D. R.; El-Baba, T. J.; Lutomski, C. A.; Trimpin, S. New Concepts for Synthetic Polymers and Additives Characterizatio. *Rapid Commun. Mass Spectrom.* **2012**, *26*, 412.
(69) Lu, I. C.; Pophristic, M.; Inutan, E. D.; McKay, R. G.; McEwen, C. N.; Trimpin, S. Simplifying the Ion Source for Mass Spectrometry. *Rapid Commun. Mass Spectrom.* **2016**, *30*, 2568−2572.
(70) Kurulugama, R.; Nachtigall, F. M.; Lee, S.; Valentine, S. J.; Clemmer, D. E. Overtone Mobility Spectrometry (Part 1): Experimental Observations. *J. Am. Soc. Mass Spectrom.* **2009**, *20*, 729−737.
(71) Manard, M. J.; Kemper, P. R. Ion Mobility Mass Spectrometry: The Design of a New High-Resolution Ion Mobility Instrument with Applications Toward Electronic-State Characterization of First-row Transition Metal Cations. *Int. J. Mass Spectrom.* **2016**, *402*, 1−11.
(72) Haler, J. R. N.; Massonnet, P.; Chirot, F.; Kune, C.; Comby-Zerbino, C.; Jordens, J.; Honing, M.; Mengerink, Y.; Far, J.; Dugourd, P.; De Pauw, E. Comparison of Different Ion Mobility Setups using Poly(ethylene oxide) PEO Polymers: Drift Tube, TIMS, and T-Wave. *J. Am. Soc. Mass Spectrom.* **2018**, *29*, 114−120.

NOTE ADDED AFTER ASAP PUBLICATION

This paper was published ASAP on June 26, 2020, with a partially corrected version. The fully corrected version was reposted on August 12, 2020.

https://dx.doi.org/10.1021/jasms.0c00045
J. Am. Soc. Mass Spectrom. XXXX, XXX, XXX−XXX